CrossMark

HEPATOBILIARY-PANCREAS

Can dual-energy CT replace perfusion CT for the functional evaluation of advanced hepatocellular carcinoma?

Sébastien Mulé[1] · Frédéric Pigneur[1] · Ronan Quelever[2] · Arthur Tenenhaus[3,4] ·
Laurence Baranes[1] · Philippe Richard[2] · Vania Tacher[1,5,6] · Edouard Herin[1] ·
Hugo Pasquier[1,5] · Maxime Ronot[7,8,9] · Alain Rahmouni[1,5] · Valérie Vilgrain[7,8,9] ·
Alain Luciani[1,5,6]

Abstract

Objectives To determine the degree of relationship between iodine concentrations derived from dual-energy CT (DECT) and perfusion CT parameters in patients with advanced HCC under treatment.

Methods In this single-centre IRB approved study, 16 patients with advanced HCC treated with sorafenib or radioembolization who underwent concurrent dynamic perfusion CT and multiphase DECT using a single source, fast kV switching DECT scanner were included. Written informed consent was obtained for all patients. HCC late-arterial and portal iodine concentrations, blood flow (BF)-related and blood volume (BV)-related perfusion parameters maps were calculated. Mixed-effects models of the relationship between iodine concentrations and perfusion parameters were computed. An adjusted p value (Bonferroni method) < 0.05 was considered significant.

Results Mean HCC late-arterial and portal iodine concentrations were 22.7 ± 12.7 mg/mL and 18.7 ± 8.3 mg/mL, respectively. Late-arterial iodine concentration was significantly related to BV (mixed-effects model F statistic (F)=28.52, $p<0.0001$), arterial BF (aBF, F=17.62, $p<0.0001$), hepatic perfusion index (F=28.24, $p<0.0001$), positive enhancement integral (PEI, F=66.75, $p<0.0001$) and mean slope of increase (F=32.96, $p<0.0001$), while portal-venous iodine concentration was mainly related to BV (F=29.68, $p<0.0001$) and PEI (F=66.75, $p<0.0001$).

Conclusions In advanced HCC lesions, DECT-derived late-arterial iodine concentration is strongly related to both aBF and BV, while portal iodine concentration mainly reflects BV, offering DECT the ability to evaluate both morphological and perfusion changes.

Key points
• *Late-arterial iodine concentration is highly related to arterial BF and BV.*
• *Portal iodine concentration mainly reflects tumour blood volume.*
• *Dual-energy CT offers significantly decreased radiation dose compared with perfusion CT.*

✉ Sébastien Mulé
    sebastien.mule@gmail.com

[1] Service d'Imagerie Médicale, AP-HP, Hôpitaux Universitaires Henri Mondor, 51 Avenue du Marechal de Lattre de Tassigny, 94010 Creteil Cedex, France

[2] GE Healthcare, 283 rue de la Minière, 78530 Buc, France

[3] Laboratoire des Signaux et Systèmes, Université Paris-Saclay, Orsay, France

[4] Biostatistics and bioinformatics core facility, Brain and Spine Institute, Paris, France

[5] Faculté de Médecine, Université Paris Est Creteil, Creteil, France

[6] INSERM IMRB, U 955, Equipe 18, Creteil, France

[7] Service de Radiologie, AP-HP, Hôpitaux Universitaires Paris Nord Val de Seine, Beaujon, 100 boulevard General Leclerc, 92118 Clichy, France

[8] Université Paris Diderot, Sorbonne Paris Cité, Paris, France

[9] INSERM U1149, centre de recherche biomédicale Bichat-Beaujon, CRB3, Paris, France

 Springer

Abbreviations

DECT	Dual-energy CT
BF	Blood flow
BV	Blood volume
aBF	Arterial blood flow
pBF	Portal blood flow
HPI	Hepatic perfusion index
MTT	Mean transit time
MSI	Mean slope of increase
PS	Capillary permeability surface product
TTP	Time to peak
PEI	Positive enhancement integral
AASLD	American Association for the Study of Liver Diseases

Introduction

Accurate evaluation of hepatocellular carcinoma (HCC) vascularity and perfusion features is of paramount importance for both early diagnosis and longitudinal follow-up under treatment, especially in advanced HCC under targeted antiangiogenic therapies [1].

Perfusion CT has been shown to provide a quantitative evaluation of tumour vascularity and angiogenesis [2, 3]. Moreover, CT perfusion-derived parameters such as blood flow (BF), blood volume (BV), mean transit time (MTT) or mean slope of increase (MSI) have been suggested to enable monitoring of tumour response to antiangiogenic treatments or local therapy [4–6] or survival prediction under antiangiogenic treatments [4] in patients with HCC. However, perfusion CT is associated with relatively high radiation dose, as multiple, repeated acquisitions of the same volume of interest are required [7].

Dual-energy CT (DECT) enables quantification of local iodine concentration [8, 9]. DECT benefits from low radiation exposure when compared with perfusion CT [10]. Iodine concentration estimated at arterial and portal-venous phases has been shown to correlate with microvessel density and to enable accurate evaluation of tumour vascular changes after antiangiogenic therapy in a rabbit liver tumour model [11]. It has been also suggested that tumour iodine uptake can be used as a biomarker of tumour vascularity and may predict tumour response to antiangiogenic therapy in patients with advanced HCC [6]. Gordic et al. recently found strong correlations between iodine density and both blood flow (BF, or total perfusion) and arterial blood flow (aBF, or arterial perfusion) in HCC using dual-source DECT [12]. Thaiss et al. found similar results with volume perfusion CT parameters, using a dual-source DECT scanner in HCC as well [13]. In both studies, a single compartment perfusion analysis using the maximum slope model was implemented for estimating perfusion parameters. This approach does not allow the estimation of

perfusion parameters such as BV, MTT, or capillary permeability surface product (PS) because it takes into account only the first part of the liver enhancement curve before venous outflow (no venous outflow assumption). Thaiss et al. additionally computed a two-compartment model with Patlak method to estimate BV within HCC lesions [13]. Moreover, arterial perfusion was estimated 9 s after abdominal aorta enhancement by Gordic et al. and 7 s after aortic peak enhancement by Thaiss et al., while a later arterial phase (i.e. around 15-20 s after abdominal aorta enhancement) may be more adapted for the detection of HCC lesions in clinical practice [14, 15].

In this context, the aim of this study was to determine whether iodine concentration values derived from late-arterial and portal-venous phases obtained with DECT were related to perfusion CT parameters calculated with a dual vascular input algorithm.

Materials and methods

Authors who were not employees of or consultants for GE Healthcare had control of inclusion of all data and information that might present a conflict of interest for those authors who are employees of or consultants for that industry. This study had local ethics and institutional review board committee approval. Written informed consent was obtained from all enrolled patients.

Study population

Between November 2012 and December 2014, 23 patients (21 men, two women; mean age 66 years ± 12, range 47-84 years) with advanced HCC were prospectively enrolled at our institution in the prospective, randomized, open-label, multicentre SARAH trial comparing radioembolization with yttrium-90 resin microspheres versus sorafenib in patients with advanced HCC according to the Barcelona criteria (stage C) or recurrent HCC after surgical or thermoablative treatment who are not eligible for surgical resection, liver transplantation or thermal ablation, or after two sessions of chemoembolization with incomplete response [16]. According to the SARAH study protocol, patients were free of extrahepatic metastasis.

All patients included in the SARAH trial underwent concurrent dynamic hepatic perfusion CT and diagnostic multiphase contrast-enhanced abdominal CT at both baseline before radioembolization or sorafenib onset, and during follow-up to monitor tumour response (n=64 from 23 patients). All CT exams among these baseline and follow-up CT exams in which diagnostic multiphase CT was performed using dual-energy technique were eligible for the present study (n=51 from 18 patients). Exclusion criteria were portal vein thrombosis preventing definition of a portal venous input for

perfusion analysis (n=5), and absence of HCC lesion (n=2) or portal branch (n=5) covered by the CT perfusion volume (Fig 1). The final study population included 39 CT datasets including both perfusion CT and diagnostic multiphase DECT acquired concurrently from 16 patients (mean age 66 years ± 11, range 44-84 years) (Fig 1, Table 1): seven CT datasets were acquired at baseline and 32 during follow-up (five at M1, 10 at M3, four at M6, three at M9, two at M12, three at M15, and five at the end of participation). The mean body weight was 76.6 kg ± 15.3 (range 49-106 kg) and the mean body mass index was 25.6 kg/m^2 ± 4.7 (range 18-34.3 kg/m^2).

According to the SARAH study protocol, a final HCC diagnosis was reached histologically or cytologically in three patients, and using AASLD criteria in 13 patients [17]. All selected HCC lesions were visually defined as hypervascular and non-hypervascular according to LI-RADS 2014 criteria [18].

CT protocol

All included patients underwent concurrent dynamic single-energy, polychromatic hepatic perfusion CT and diagnostic multiphase abdominal contrast-enhanced DECT at baseline and during follow-up using a 64-section single-source DECT scanner (Discovery HD 750; GE Healthcare, Milwaukee, WI, USA). First, a non-enhanced low-dose CT of the abdomen was performed, and a scan volume of 40 mm on the z-axis was placed to cover the largest HCC lesions and the portal vein. According to the SARAH study protocol, perfusion CT had to be performed before diagnostic multiphase DECT, as perfusion CT is acquired with a limited volume of contrast material. For each patient, 40 mL of non-ionic

contrast material (iomeprol, 400 mg iodine/mL; Iomeron 400, Bracco Imaging, Milano, Italy) was injected into an antecubital vein at a flow rate of 5 mL/s followed by 20 mL of saline solution at the same flow rate. As soon as the injection started, 40 mm large acquisitions were repeatedly performed every second during 30 s, and every three seconds during the following 90 s, leading to a total of 60 volume acquisitions and a total examination time of 120 s. Scan parameters were tube voltage, 80 kVp; tube current, 100 mA; tube current-time product, 100 mAs; section collimation, 64 × 0.6 mm. Patients were instructed to breathe freely during the perfusion scan. Perfusion images were reconstructed with a section thickness of 5 mm.

Ten minutes after the end of the perfusion images acquisition, a multiphasic abdominal DECT was performed using the same CT scanner. An additional volume of an identical contrast material was injected at a flow rate of 5 mL/s. The volume was defined as 2 mL/kg body weight minus the 40 mL already used for perfusion CT. Bolus tracking software (Smartprep, GE Healthcare, WI, USA) was used and late-arterial and portal phases were acquired respectively 20 s after the attenuation increase in abdominal aorta reached the predefined threshold of 80 HU and 40 s thereafter. A delayed phase acquisition encompassing the entire liver was acquired at a 3 min delay. Acquisition parameters were as follows: tube voltage pair, 80 kVp and 140 kVp; tube current-time, 277 mAs; section collimation, 64 × 1.25 mm; scan time per spiral, 0.5 s. DECT images were reconstructed with a section thickness of 5 mm in order to be consistent with the 5 mm-thickness of perfusion CT images. Radiation exposure associated with both perfusion CT and DECT scans was investigated; the dose-length product (DLP, mGy.cm) and volume CT

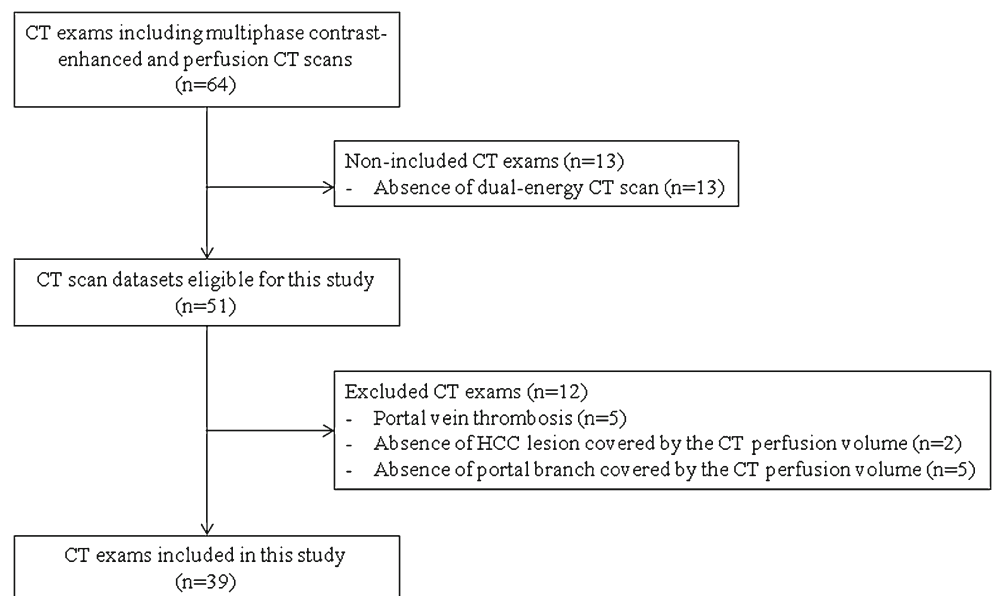**Fig. 1** Flow chart of study enrolment. Inclusion and exclusion criteria are provided

Springer

Table 1 Patients Demographics

Variable	Population (n=16)
Sex	
Male	14
Female	2
Age (years)	66 ± 11
BMI (kg/m2)	25.6 ± 4.7
ECOG performance status	
0	9
1	7
Cause of disease	
Chronic hepatitis B only	3
Chronic hepatitis C only	2
Alcohol only	2
Chronic hepatitis C + alcohol	3
Metabolic syndrome	3
Metabolic syndrome + alcohol	1
Other	2
Child-Pugh class	
A5	9
A6	4
B7	3
HCC type	
Nodular	11
Infiltrative	5
Macroscopic vascular invasion	10
Treatment	
Sorafenib	9
Radioembolisation	7
Biochemical analysis	
Albumin (g/dL)	36 ± 8
Total bilirubin (mg/dL)	16 ± 9
Alpha-fetoprotein (ng/mL)	1373 ± 4220

dose index (CTDI$_{vol}$, mGy) values of both perfusion CT and DECT (late-arterial and portal venous phases) series were systematically collected.

Perfusion CT and DECT quantitative analysis

All CT exams were transferred to a commercially available workstation (Advantage Workstation server 3.2, GE Healthcare) and post-processing was performed by using dedicated software (CT perfusion 4D, GE Healthcare). A non-rigid, deformable motion correction algorithm was first applied on all perfusion CT images in order to prevent any motion artefact. Then, two circular regions of interest (ROIs) were manually placed in the abdominal aorta and the portal vein to provide both arterial and portal input functions by two radiologists separately, with respective 15 years (R1) and 8 years (R2) in abdominal imaging (Fig 2). Liver perfusion was calculated by using a deconvolution model with a dual vascular input algorithm [19], allowing the estimation of the following perfusion parameters: BF (mL/100 g/min), BV (mL/100 g), aBF (mL/100 g/min), portal BF (pBF, mL/100 g/min), hepatic perfusion index (HPI, %), MTT (s), time to peak (TTP, s), PS (%), MSI (HU/s), and positive enhancement integral (PEI, %). Radiologists R1 and R2 independently selected on the perfusion CT images providing the highest visual liver-to-lesion contrast the section with the largest cross-sectional area of the HCC lesions and placed free-hand ROIs encompassing the entire HCC lesions, including necrotic areas (mean size, 6.5 cm^2 ± 8.2). In case of multifocal HCC, ROIs were positioned on the two largest lesions. An additional circular ROI was placed on tumour-free liver parenchyma, avoiding inclusion of large hepatic vessels (mean size, 4.2 cm^2 ± 3.0) away from the HCC lesions, optimally in the contralateral hemiliver in case of HCC single hemiliver involvement in order to limit potential radioembolization-related perfusion variations. All ROIs were then automatically copied at the same location on the other perfusion parametric maps

Fig. 2 Axial (a) arterial and (b) portal perfusion CT images show circular ROIs manually placed on the abdominal aorta (ROI1) and the portal vein (ROI2) to enable perfusion parameters to be calculated, a free-hand ROI encompassing the HCC lesion (ROI4) and an additional circular ROI (ROI3) in the tumour-free liver parenchyma
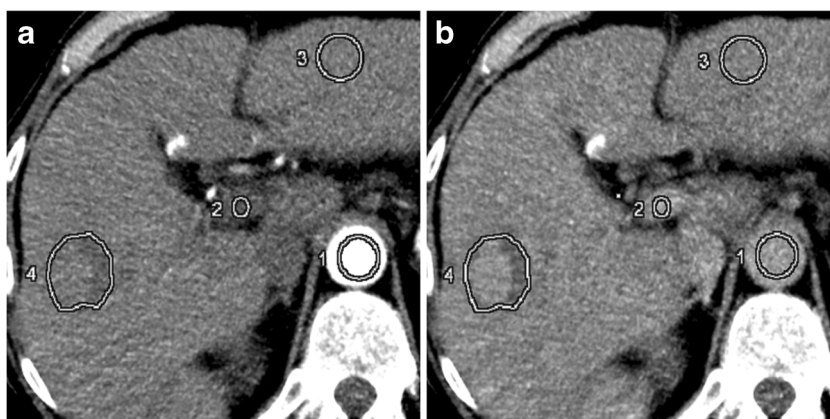
(Clone® tool, Advantage Workstation server 3.2, GE Healthcare).

Iodine concentration maps at the late-arterial and portal-venous phases were automatically generated from DECT images (GSI viewer, GE Healthcare). Iodine concentrations in HCC lesions were semi-automatically calculated. Manually placed free-hand ROIs previously defined on perfusion maps were automatically copied on iodine concentration maps, preventing any difference in ROIs size and shape. Readers additionally adjusted ROIs placement to take into account the respiratory misregistration that may occur between perfusion CT and diagnostic multiphase DECT scans. Finally, averaged late-arterial and portal iodine concentrations (mg/100 g of liver) were automatically calculated in each ROI.

Statistical analysis

Continuous variables were expressed as mean ± standard deviation. Variables were assessed for normal distribution by using the Shapiro-Wilks test. The Student's t-test was used to compare perfusion parameters and iodine concentration values in HCC lesions and tumour-free liver parenchyma. The interreader agreement for the estimations of perfusion parameters and iodine concentrations was assessed using intraclass correlation coefficients (ICC) for each pair of variables. Because perfusion parameters and iodine concentrations were measured in potentially multiple lesions for each patient, and at different times (at baseline and/or during follow-up), our data were not independent. Therefore, the relationship between each parameter and late-arterial and portal iodine concentrations was evaluated by using linear mixed-effects models, with patient and lesion as random effects and time and the considered perfusion parameter as fixed effects.

Iodine concentrations were the explained variables. A Bonferroni correction was performed to address the multiple comparisons. The significance of the models was determined with the mixed-model F statistic and two-sided adjusted p-values <0.05. Statistical analyses were performed using the computing environment R 3.0.1 (R Development Core Team, 2013).

Results

Perfusion CT and DECT quantitative analysis

From the 39 included CT exams, a total of 50 HCC lesions were selected for analysis (mean largest cross-sectional diameter, 30.2 mm ± 26). Thirty-two HCC lesions demonstrated hypervascular profile, and 18 HCC lesions were non-hypervascular. Analysis of perfusion CT-derived parameters showed significantly higher aBF ($p<0.001$), HPI ($p<0.001$), PS ($p=0.020$) and MSI ($p<0.0012$), and significantly lower BV ($p=0.015$), pBF ($p<0.001$), TTP ($p=0.0093$) and PS ($p=0.035$) in HCCs when compared with tumour free liver parenchyma (Table 2). Late-arterial iodine concentration was significantly higher in HCCs than in liver parenchyma ($p=0.034$) (Table 2). An example of perfusion and iodine concentration parametric maps is shown in Fig 3.

Strong interreader agreement was found for all perfusion CT parameters in HCC lesions (ICC values from 0.77 for pBF up to 0.90 for aBF, BV, TTP and MTT). Interreader agreement was also strong for late-arterial and portal-venous iodine concentrations within HCC lesions (ICC values of 0.82 and 0.75, respectively). In tumour-free liver parenchyma, interreader agreement was strong for all perfusion parameters (ICC values

Table 2 Perfusion CT-Derived Parameters and Dual-Energy CT-Derived Iodine Concentrations

CT parameter	HCC	Tumor Free Liver Parenchyma	p value
Perfusion CT			
Blood Flow (mL/100 g/min)	93.8 ± 89.4	118.3 ± 92.9	0.067
Blood Volume (mL/100 g)	24.0 ± 13.2	30.1 ± 7.2	0.015*
Arterial Blood Flow (mL/100 g/min)	58.0 ± 41.7	14.1 ± 13.0	< 0.001*
Portal Blood Flow (mL/100 g/min)	37.0 ± 68.6	105.1 ± 96.6	< 0.001*
Hepatic Perfusion Index (%)	0.7 ± 0.3	0.2 ± 0.3	< 0.001*
Mean Transit Time (s)	23.0 ± 11.2	23.0 ± 11.2	0.66
Time to Peak (s)	37.9 ± 28.7	54.4 ± 19.9	0.0093*
Permeability Surface Area Product (%)	3.2 ± 4.9	1.5 ± 3.6	0.020*
Positive Enhanced Integral (HU/s)	0.3 ± 0.2	0.3 ± 0.1	0.83
Mean Slope of Increase (%)	2.3 ± 1.9	0.9 ± 0.5	0.0012*
Dual-energy CT			
Arterial Iodine Concentration (mL/100 g)	22.7 ± 12.6	17.1 ± 5.2	0.034*
Portal Iodine Concentration (mL/100 g)	18.7 ± 8.5	24.5 ± 6.5	0.089

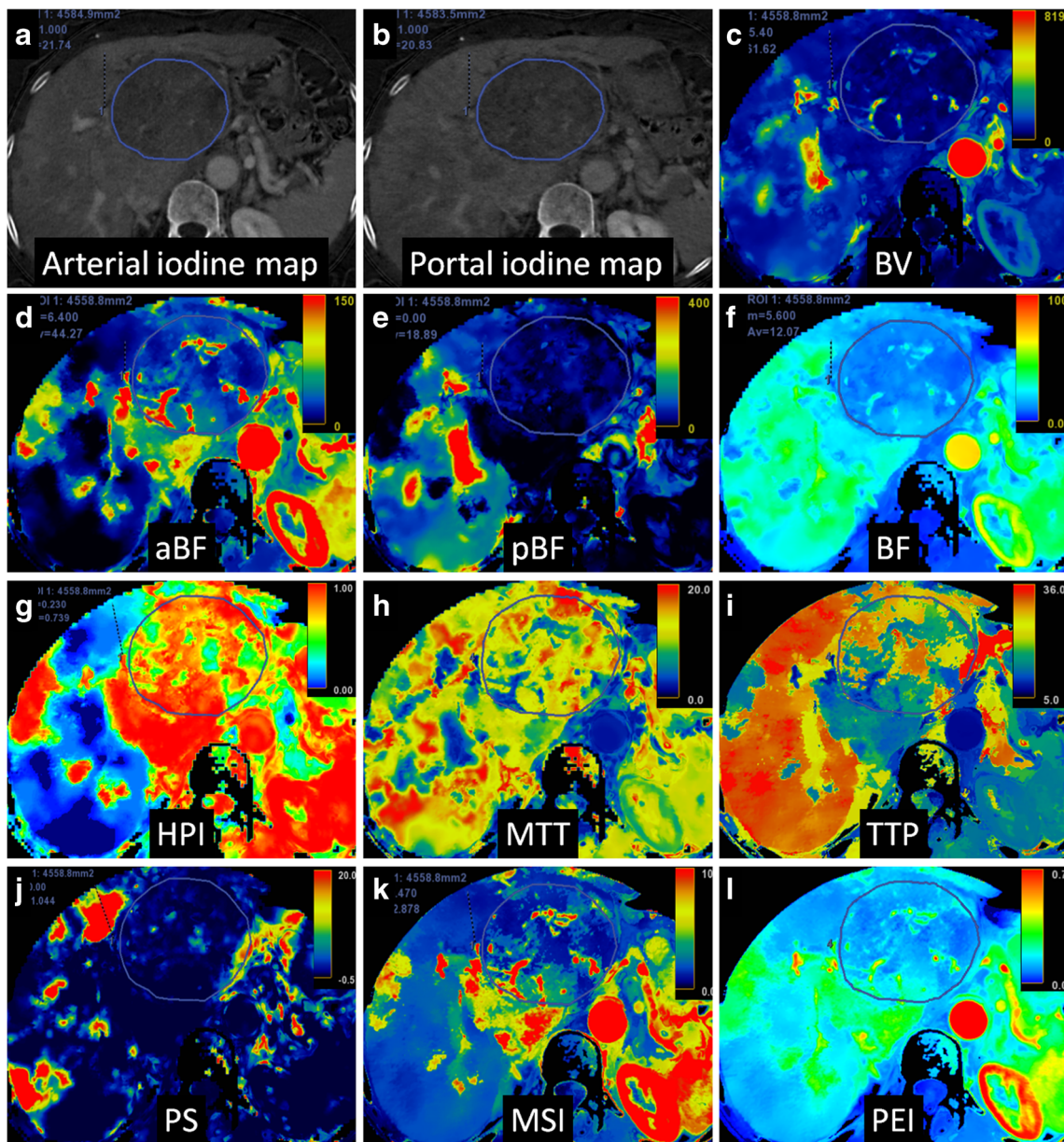*Indicates a significant correlation

Fig. 3 CT images in a 64-year-old man with HCC in the right liver lobe. Axial images of iodine concentration at (a) the late-arterial phase and (b) the portal phase derived from multiphasic contrast-enhanced dual-energy CT. Axial parametric maps of (c) blood volume (BV), (d) arterial blood flow (aBF), (e) portal blood flow (pBF), (f) blood flow (BF), (g) hepatic perfusion index (HPI), (h) mean transit time (MTT), (i) time to peak (TTP), (j) permeability surface area product (PS), (k) mean slope of increase (MSI) and (l) positive enhancement integral (PEI) calculated from perfusion CT. The low late-arterial and portal iodine concentrations in the outlined HCC lesion when compared with the lesion-free liver parenchyma are associated with low values of BV, pBF and BF, TTP, and high values of HPI and aBF

from 0.73 for MTT to 0.89 for aBF and HPI), and for late-arterial and portal iodine concentrations (ICC values of 0.88 and 0.87, respectively). As a result, only values observed by the most experienced reader in abdominal radiology (R1) were used for further correlation analysis.

The mean radiation dose of hepatic perfusion CT and DECT (late-arterial and portal venous phases) were DLP, 324.4 mGy.cm and 1113.1 ± 87.8 mGy.cm, respectively, and CTDI$_{vol}$, 81.1 mGy and 10.8 ± 1.2 mGy, respectively.

Statistical relationship between Perfusion CT and DECT

Linear mixed-effects model analysis revealed that late-arterial and portal-venous iodine concentrations were significantly related to BV (respectively F=28.52, $p<0.0001$, and F=29.68, $p<0.0001$), HPI (respectively F=28.24, $p<0.0001$, and F=11.49, $p=0.0070$), PEI (respectively F=66.75, $p<0.0001$, and F=39.93, $p<0.0001$), and MSI (respectively F=32.96, $p<0.0001$, and F=14.30, $p=0.0016$). Late-arterial iodine

concentration was also significantly associated with aBF (F=17.62, $p<0.0001$). A significant negative relationship was found between TTP and late-arterial iodine concentration (F=22.11, $p<0.0001$). Relationship estimates calculated with a mixed-effects model between late-arterial and portal iodine concentrations and perfusion CT parameters in HCC lesions are summarized in Table 3.

In tumour-free liver parenchyma, MSI was significantly related to late-arterial iodine concentration (F=18.19, $p=0.00020$). Conversely, no significant relationship was found between perfusion CT parameters and portal iodine concentration.

Discussion

The results of our study, performed in advanced HCC, suggest that late-arterial iodine concentration derived from a single source, fast kV-switching DECT is strongly related to perfusion parameters related to aBF and to BV, while portal iodine concentration mainly reflects BV. Therefore, combined analysis of variations of both late-arterial and portal iodine concentrations in HCC lesions may be helpful to evaluate perfusion changes of HCC treated with targeted or liver-directed therapy. The radiation dose by volume (CTDI$_{vol}$) of DECT is considerably lower than that of perfusion CT.

DECT is a potentially unique imaging modality providing images for both routine diagnostic purposes (i.e. multiphasic contrast-enhanced images) and for functional evaluation purposes (i.e. material-specific images such as iodine maps).

DECT has been recently suggested to allow accurate estimates of BF in HCC lesions [12, 13]. However, BF parameters were estimated using a single compartment analysis using the maximum slope model, which makes the assumption of no venous outflow and may, therefore, lead to underestimation of BF values. This was supported by the work of Kaufmann et al. who found lower estimated BF values when computing compartmental analysis using the maximum slope model than that estimated with deconvolution analysis in HCC lesions [20]. In the present study, a deconvolution model using a dual vascular input algorithm was used. Values of BF within HCC lesions were higher than those obtained by the two aforementioned studies, with mean BF, aBF and pBF values of 93.8, 58.0, and 37.0 mL/100 g/min, respectively, versus 72.4, 53.0, and 23.4 mL/100 mL/min, respectively, found by Gordic et al., and 52.2, 44.4, and 9.6 mL/100 mL/min, respectively, found by Thaiss et al. study [12, 13]. Moreover, the higher sensitivity to image noise of compartmental analysis when compared with deconvolution analysis may additionally reduce the accuracy of estimated BF values, especially in cases of low BF values [21].

Estimated BV values (mean value of 24.0 mL/100 g) were in line with those previously found by Ippolito et al. (median value of 20.4 mL/100 mL), but higher than those found by Thaiss et al. (mean value of 13 mL/100 mL) or Sahani et al. (mean value of 4.9 mL/100 g). The discrepancy with the study of Thaiss et al. may be explained by the too low temporal resolution of one helical cycle time per 3.5 s chosen in the latter study. Indeed, Ng et al. recently showed that increasing the cycle time beyond

Table 3 Relationship estimates calculated with mixed-effects models between dual-energy CT-derived iodine concentrations and perfusion CT parameters in HCC lesions

Perfusion CT parameter	Arterial Iodine Concentration			Portal Iodine Concentration		
	Coefficient	F	p value	Coefficient	F	p value
Blood Flow (mL/100 g/min)	2.08	1.47	1	2.50	1.65	1
Blood Volume (mL/100 g)	0.82	28.52	<.0001*	1.22	29.68	<.0001*
Arterial Blood Flow (mL/100 g/min)	2.25	17.62	<.0001*	1.90	7.52	0.061
Portal Blood Flow (mL/100 g/min)	-0.71	0.74	1	-0.088	0.01	1
Hepatic Perfusion Index (%)	0.018	28.24	<.0001*	0.020	11.49	0.0070*
Mean Transit Time (s)	0.066	0.26	1	0.25	1.82	1
Permeability Surface Area Product (%)	-0.071	1.87	1	0.018	0.07	1
Time to Peak (s)	-1.64	22.11	<.0001*	-1.37	7.02	0.081
Positive Enhancement Integral (%)	0.010	66.75	<.0001*	0.012	39.93	<.0001*
Mean Slope of Increase (HU/s)	0.11	32.96	<.0001*	0.11	14.30	0.0016*

Estimates of coefficient, F and adjusted p value (Bonferroni method), respectively, reflect the strength, sign and degree of statistical significance of the association

*Indicates a significant correlation

1 s significantly affects CT perfusion parameters values in neuroendocrine liver metastases, and that the higher the cycle time value, the higher the difference in perfusion parameters estimates [22]. A cycle time of 1 s was used in the present study during the early perfusion phase, in accordance with recent guidelines [23]. The choice of the perfusion model (i.e. compartment model vs deconvolution model) may also have contributed to the differences of BV estimates between the study of Thaiss et al. and the present study. Djuric-Stefanovic et al. founded significantly different perfusion CT parameters values with the deconvolution and maximum slope algorithms in esophageal cancers, although they correlated significantly with each other [24]. The discrepancy with the study of Sahani et al. may be due to the different duration of perfusion CT acquisitions (25 or 30 s vs. 120 s in the present study), which has been proven to significantly affect perfusion CT parameter values in liver lesions [25].

Relationship between BV and iodine concentration in HCC has seldom been investigated in humans. Thaiss et al. recently found a moderate correlation between BV and arterial iodine concentration (r=0.60). In the present study, highly significant relationship estimates were found between BV-related perfusion parameters (i.e., BV, PEI) and both late-arterial and portal iodine concentrations. Several factors may have contributed to this significant relationship between BV and iodine concentration. First, as previously mentioned, acquisition parameters were different in the present study, with higher temporal resolution of perfusion CT during the arterial phase (cycle time of 1 s vs. 3.5 s) and longer acquisition duration (120 s vs. 40 s). Second, the timing of the DECT arterial phase acquisition differed: late-arterial DECT acquisition was initiated 20 s after preset threshold value of 80 HU within the abdominal aorta, while Thaiss et al. chose a scan delay of 7 s after peak aortic enhancement, which may be too early to accurately depict wash-in associated with HCC lesions [15] and may also not be applicable to clinical practice, as patient-specific arterial peak enhancement could not be known prior to starting DECT acquisition. Third, Thaiss et al. estimated iodine concentrations from perfusion CT datasets using *in vitro* calibration measurements performed with phantoms, which may differ from iodine concentrations calculated using a DECT protocol as performed in the present study. Finally, patient body habitus may impact on iodine concentration quantification. In the present study, the observed BMI values were in line with standard values in European populations [26].

Perfusion CT analysis was performed with a deconvolution model using a dual vascular input algorithm. As HCC lesions classically appear hypervascular at the arterial phase due to both hyperarterialization and decreased portal flow, the use of a model with a single arterial input may be discussed. However, taking into account the tumour portal supply in a model with a dual vascular input algorithm has been suggested to yield more precise evaluation of CT perfusion parameters [27].

Some limitations of this study should be noted. First, the number of included patients and datasets is small. However, all data were acquired prospectively in an ongoing randomized trial comparing radioembolization with sorafenib in advanced HCC. Our results must be further investigated with a large patient cohort. Second, the same DECT protocol was used for all patients, regardless of clinical characteristics of patients such as bodyweight or BMI. Notably, modulation of tube current-time product was not performed. Indeed, fast kV-switching DECT technology does not allow tube current modulation. Third, the cranial-caudal liver volume explored by perfusion CT was 4 cm, i.e. the lower limit of recommended z-axis coverage [23]. This may lead to bias of selection, as lesions away from the portal vein could not be analysed. More recent CT scanners allow wider z-axis coverage up to 16 cm and the performance of 16 cm perfusion CT could probably be greatly improved. Last, included patients followed different therapeutic regimens, whether using antiangiogenics or radioembolization; however, the primary aim of this study was not to address treatment response, but rather to investigate for each examination performed the relationship between perfusion parameters and DECT-derived iodine concentrations within tumours. Dynamic contrast-enhanced MRI has also been used to monitor early response to treatment [28]. Further studies comparing DECT and dynamic contrast-enhanced MRI should be conducted. In conclusion, in advanced HCC lesions, DECT-derived late-arterial iodine concentration is strongly related to both aBF and BV, while portal iodine concentration mainly reflects lesion BV, offering DECT the ability to evaluate both morphological and perfusion changes.

Informed consent Written informed consent was obtained from all patients in this study.

Ethical approval Institutional Review Board approval was obtained.

Methodology
• prospective
• cross sectional study
• performed at one institution

References

1. Miles KA (2003) Functional CT imaging in oncology. Eur Radiol 13:M134–M138

2. Sahani DV, Holalkere NS, Mueller PR, Zhu AX (2007) Advanced hepatocellular carcinoma: CT perfusion of liver and tumor tissue– initial experience. Radiology 243:736–743

3. Ippolito D, Capraro C, Casiraghi A, Cestari C, Sironi S (2012) Quantitative assessment of tumour associated neovascularisation in patients with liver cirrhosis and hepatocellular carcinoma: role of dynamic-CT perfusion imaging. Eur Radiol 22:803–811

4. Jiang T, Kambadakone A, Kulkarni NM, Zhu AX, Sahani DV (2012) Monitoring response to antiangiogenic treatment and predicting outcomes in advanced hepatocellular carcinoma using image biomarkers, CT perfusion, tumor density, and tumor size (RECIST). Invest Radiol 47:11–17

5. Ippolito D, Fior D, Bonaffini PA et al (2014) Quantitative evaluation of CT-perfusion map as indicator of tumor response to transarterial chemoembolization and radiofrequency ablation in HCC patients. Eur J Radiol 83:1665–1671

6. Dai X, Schlemmer HP, Schmidt B et al (2013) Quantitative therapy response assessment by volumetric iodine-uptake measurement: initial experience in patients with advanced hepatocellular carcinoma treated with sorafenib. Eur J Radiol 82:327–334

7. Kim SH, Kamaya A, Willmann JK (2014) CT perfusion of the liver: principles and applications in oncology. Radiology 272:322–344

8. Marin D, Boll DT, Mileto A, Nelson RC (2014) State of the art: dual-energy CT of the abdomen. Radiology 271:327–342

9. Matsumoto K, Jinzaki M, Tanami Y, Ueno A, Yamada M, Kuribayashi S (2011) Virtual monochromatic spectral imaging with fast kilovoltage switching: improved image quality as compared with that obtained with conventional 120-kVp CT. Radiology 259:257–262

10. Stiller W, Skornitzke S, Fritz F et al (2015) Correlation of quantitative dual-energy computed tomography iodine maps and abdominal computed tomography perfusion measurements: are single-acquisition dual-energy computed tomography iodine maps more than a reduced-dose surrogate of conventional computed tomography perfusion? Invest Radiol 50:703–708

11. Lv P, Liu J, Yan X et al (2017) CT spectral imaging for monitoring the therapeutic efficacy of VEGF receptor kinase inhibitor AG-013736 in rabbit VX2 liver tumours. Eur Radiol 27:918–926

12. Gordic S, Puippe GD, Krauss B et al (2016) Correlation between Dual-Energy and Perfusion CT in Patients with Hepatocellular Carcinoma. Radiology 280:78–87

13. Thaiss WM, Haberland U, Kaufmann S et al (2016) Iodine concentration as a perfusion surrogate marker in oncology: Further elucidation of the underlying mechanisms using Volume Perfusion CT with 80 kVp. Eur Radiol 26:2929–2936

14. Kagawa Y, Okada M, Yagyu Y et al (2013) Optimal scan timing of hepatic arterial-phase imaging of hypervascular hepatocellular carcinoma determined by multiphasic fast CT imaging technique. Acta Radiol 54:843–850

15. Hammerstingl RM, Vogl TJ (2005) Abdominal MDCT: protocols and contrast considerations. Eur Radiol 15:E78–E90

16. Vilgrain V, Abdel-Rehim M, Sibert A et al (2014) Radioembolisation with yttrium90 microspheres versus sorafenib for treatment of advanced hepatocellular carcinoma (SARAH): study protocol for a randomised controlled trial. Trials 15:474

17. Bruix J, Sherman M (2011) Management of hepatocellular carcinoma: an update. Hepatology 53:1020–1022

18. American College of Radiology. Liver Imaging Reporting and Data System version 2014. Available via http://www.acr.org/Quality-Safety/Resources/LIRADS. Accessed April 2016

19. St Lawrence KS, Lee TY (1998) An adiabatic approximation to the tissue homogeneity model for water exchange in the brain: I. Theoretical derivation. J Cereb Blood Flow Metab 18:1365–1377

20. Kaufmann S, Horger T, Oelker A et al (2015) Characterization of hepatocellular carcinoma (HCC) lesions using a novel CT-based volume perfusion (VPCT) technique. Eur J Radiol 84:1029–1035

21. Miles KA (2003) Perfusion CT for the assessment of tumour vascularity: which protocol? Br J Radiol 76:S36–S42

22. Ng CS, Hobbs BP, Wei W et al (2015) Effect on perfusion values of sampling interval of computed tomographic perfusion acquisitions in neuroendocrine liver metastases and normal liver. J Comput Assist Tomogr 39:373–382

23. Miles KA, Lee TY, Goh V et al (2012) Current status and guidelines for the assessment of tumour vascular support with dynamic contrast-enhanced computed tomography. Eur Radiol 22:1430–1441

24. Djuric-Stefanovic A, Saranovic D, Masulovic D, Ivanovic A, Pesko P (2013) Comparison between the deconvolution and maximum slope 64-MDCT perfusion analysis of the esophageal cancer: is conversion possible? Eur J Radiol 82:1716–1723

25. Ng CS, Hobbs BP, Chandler AG et al (2013) Metastases to the liver from neuroendocrine tumors: effect of duration of scan acquisition on CT perfusion values. Radiology 269:758–767

26. NCD Risk Factor Collaboration (2016) Trends in adult body-mass index in 200 countries from 1975 to 2014: a pooled analysis of 1698 population-based measurement studies with 19.2 million participants. Lancet 387:1377–1396

27. Ng CS, Chandler AG, Wei W et al (2012) Effect of dual vascular input functions on CT perfusion parameter values and reproducibility in liver tumors and normal liver. J Comput Assist Tomogr 36:388–393

28. Chen BB, Hsu CY, Yu CW et al (2017) Early perfusion changes within 1 week of systemic treatment measured by dynamic contrast-enhanced MRI may predict survival in patients with advanced hepatocellular carcinoma. Eur Radiol 27:3069–3079